# The Ottana solar facility: dispatchable power from small-scale CSP plants based on ORC systems

Mario Petrollese,* Giorgio Cau, Daniele Cocco
Department of Mechanical, Chemical and Materials Engineering, University of Cagliari, Via Marengo, 2 09123 Cagliari, Italy.
* Corresponding Author: Mario Petrollese
petrollese@unica.it, Tel. ++39 070 6755741 Fax. ++39 070 6755717

**Abstract**

The Ottana solar facility aims to demonstrate the capabilities of concentrating solar technologies to provide dispatchable power and ancillary services at distribution level. The facility includes a 630 kW Concentrating Solar Power (CSP) plant with thermal storage coupled with a 400 kW Concentrating Photovoltaic (CPV) plant with electrochemical storage. The CSP+CPV plant aims to study the ability of the integrated concentrating solar systems to deliver scheduled power profiles for the following day on the basis of weather forecasting data. The CSP section is based on linear Fresnel collectors using thermal oil as heat transfer fluid and a two-tank direct Thermal Energy Storage (TES) system with a storage capacity of about 15 $MWh_t$. The power generation is carried out by a 630 kW Turboden 6HR Special ORC unit. This paper focuses on a description of the CSP plant section and on the analysis of its expected performance. In particular, the control strategy developed for determining the daily power profiles starting from the weather forecasting data is presented. Moreover, the first operating results and the expected performance of the CSP plant are reported and discussed.

**Keywords:** Solar ORC; Concentrating solar power; Linear Fresnel collectors; Thermal energy storage

**NOMENCLATURE**

***Symbols***

| | |
|---|---|
| $A_{SF}$ | Solar field collecting area [m$^2$] |
| $E_{DEF}$ | Annual defocusing losses [MWh$_t$/year] |
| $E_{EL}$ | Annual electricity production [MWh/year] |
| $E_{HT}$ | Stored energy in the hot tank [MWh$_t$] |
| $\widetilde{E}_{IN}$ | Expected overall daily thermal energy input [MWh$_t$/day] |
| $E_{SF}$ | Actual daily solar field energy production [MWh$_t$/day] |
| $E_{UN}$ | Annual undelivered electrical energy [MWh/year] |
| $\widetilde{E}_{SF}$ | Expected daily solar field energy production [MWh$_t$/day] |
| $FL_{HT}$ | Hot tank filling level |
| $FL_{MIN}$ | Minimum filling level |
| $M_{HT}$ | Oil mass stored in hot tank [kg] |
| $M_{HT,MAX}$ | Maximum oil mass stored in hot tank [kg] |
| $P_{EL}$ | ORC net electrical power [MW] |
| $P_{EL,MIN}$ | Minimum ORC net electrical power [MW] |
| $\dot{Q}_{DEF}$ | Solar field defocusing losses [MW] |
| $\dot{Q}_{L,TH}$ | Solar field thermal losses [MW] |
| $\dot{Q}_{PB}$ | Power block thermal power input [MW] |
| $\dot{Q}_{SF}$ | Solar field thermal power production [MW] |
| $T_{AMB}$ | Ambient temperature [°C] |
| $T_{HT}$ | Hot tank average temperature [°C] |
| $t_{ON}$ | ORC start-up time [h] |
| $\eta_{OPT}$ | Solar field optical efficiency |
| $\eta_{ORC}$ | Organic Rankine cycle efficiency |
| $\tau_{CPV}$ | CPV delivery period [h] |
| $\tau_{ORC}$ | ORC delivery period [h] |
| $\tau_{ORC,MIN}$ | Minimum ORC delivery period [h] |

***Acronyms***

| | |
|---|---|
| CPV | Concentrating photovoltaic |
| CSP | Concentrating solar power |
| DNI | Direct normal irradiance |
| LFC | Linear Fresnel collector |
| HTF | Heat transfer fluid |
| ORC | Organic Rankine cycle |
| PB | Power block |
| PTC | Parabolic trough collector |
| PB | Power block |
| PV | Photovoltaic |
| RES | Renewable energy source |
| SF | Solar field |
| TES | Thermal energy storage |

## 1 Introduction

Nowadays, two mature and commercial technologies are available for the electricity generation from solar energy: (1) Photovoltaic (PV) systems, which are the most widespread technology (176 GW of installed capacity in 2014), and (2) Concentrating Solar Power (CSP), with 5 GW of overall electrical capacity in 2014 [1]. Generally, CSP systems are characterized by higher capital costs compared to PV system. Furthermore, only the direct component of the solar radiation can be exploited by CSP system, making this technology profitable and competitive only in locations with high Direct Normal Irradiance (DNI) availability [2]. On the other hand, the inclusion of a Thermal Energy Storage (TES) system makes the operability of CSP plants comparable with conventional and dispatchable power plants [3]. In fact, thermal energy can be stored for later use at relatively low costs compared to batteries (commonly used in PV systems) [4]. Moreover, the introduction of a TES section allows to partially separate the electrical power generation phase and the solar thermal power production [5], coping uncertainty in solar energy availability, mitigating short load fluctuations and shifting or extending the electricity supply period [6]. Accordingly, the role of CSP plants is different and partly complementary to PV systems, especially in a future perspective, where a high penetration of Renewable Energy Source (RES) technologies in the electric power grid is expected [7]. In this scenario, CSP technologies may deliver a flexible power generation and provide several electricity ancillary services at distribution level, such as frequency and voltage support to stabilize the power grid [8].

CSP technology is mainly adopted in large-scale plants: worldwide, solar power plants in operation are characterized by an average power output of 33 MW, which increases to 126 MW for plants in project [9]. The most common and competitive power generation cycle adopted for the solar thermal energy conversion into electricity is the Rankine cycle. Water is the most suitable and chosen working fluid for large-scale power plants operating with high temperature energy sources (>370°C). However, the use of steam for exploiting low temperature energy sources and/or low power outputs results in an inefficient and unprofitable solution, since the steam thermodynamic properties lead to the use of multistage turbines and complex plant schemes as well as to liquid phase formation during the expansion [10]. Conversely, the use of Organic Rankine Cycle (ORC) power plants, employing organic working fluids with low boiling points, leads to higher efficient and economically attractive solutions for power generation from low-grade heat sources. For this reason, ORC power systems should be considered the most suitable solution to convert solar thermal energy into electricity at a distributed scale, which usually require low-concentration collectors and power outputs from a few kW to a few MW [11].

The integration of concentrating solar collectors with ORC plants is largely studied in literature [12]. Most of these scientific works concern design optimization, selection of proper working fluids, energy and exergy analyses under design conditions [13–19]. However, the operating conditions of the ORC system are often far from the design performance, in particular in solar applications where the availability of solar energy fluctuates in time and season. For this reason, off-design performance analyses of ORC power plants are also present in literature [20–25]. Related to solar applications, He et al. [20] developed a simulation model of a parabolic trough solar thermal power generation system integrated with an ORC plant and system performance were analysed considering four typical days. Wang et al. [22] investigated the performance of a 250 kW ORC coupled with compound parabolic collectors under off-design conditions due to the fluctuations of ambient temperature and mass flow rate of Heat Transfer Fluid (HTF). Calise et al. [23] simulated the off-design performance of an ORC fed by medium-temperature heat sources (155–185°C) using n-butane as working fluid and, after a design optimization of some geometrical parameters of the shell and tube heat exchangers.

However, the operating strategy of the overall CSP-ORC power system is often a neglected aspect, although it greatly influences the reliability and profitability of the plant. In case of small-scale solar ORC systems, as those analysed in [26–28], the ORC power generation is completely devoted to cover the corresponding load demand, and the TES system, if present, is used to face some perturbations such as a cloud passing or a low temperature of the HTF loop. By referring to medium-size systems, the main objective is generally related to the maximization of the energy production, the HTF is directly sent to the power block, which often operates in off-design conditions, and only the surplus is diverted toward the storage system [29]. In alternative, as proposed in [30], the thermal storage could be privileged and the power block operation is postponed when the TES is completely charged. The simplicity in the standard practises adopted in operating strategy is mainly due to a limited baggage of operational experience and knowledge of system potentiality.

*Table 1 – CSP-ORC power plants with a power output in the range 50kW-5MW.*

| Plant (date) | Country | Collector type | Collecting area [m²] | HTF | Operating temperature [°C] | ORC system (backup) | Power output [MW] | TES type (capacity) | Ref. |
|---|---|---|---|---|---|---|---|---|---|
| Saguaro Power Plant (2006) | USA (AZ) | PTC | 10340 | Xceltherm 600 | 300/248 | Ormat (solar only) | 1 | None | [31] |
| Lafayette Plant (2012) | USA (LA) | PTC | 1051 | Water | 121/93 | ElectraTherm (solar only) | 0.05 | Buffer | [32] |
| Airlight Energy Baha Plant (2014) | Morocco | PTC | 6160 | Air | 570/270 | Turboden 18 HR (solar+waste heat) | 2 | Packed-bed of rocks (5 h) | [33] |
| Rende-CSP Plant (2014) | Italy | LFC | 9780 | Mineral oil | 280 | n.a. (solar-biomass) | 1 | None | [34] |
| Tampa Plant (2014) | USA (FL) | PTC | 1021 | Glycol | 116/77 | ElectraTherm (solar only) | 0.05 | PCM | [35] |
| Archimede (2015) | Italy | PTC | 8000 | Thermal oil | 305/204 | Turboden 12 HRS (Gas boiler) | 1 | Direct (1 h) | [36] |
| Stillwater Geo-Solar Plant (2015) | USA (NV) | PTC | 24778 | Water | n.a. | Isobutane units (Solar-Geothermal) | 2 of 35 | None | [37] |
| Aalborg CSP-Brønderslev (2016) | Denmark | PTC | 26929 | n.a. | 312/252 | Turboden 40 CHPRS split (solar-biomass) | 3.8 | None | [38] |
| Ottana solar facility (2017) | Italy | LFC | 8592 | Thermal oil | 275/165 | Turboden 6HR Special (solar-only) | 0.6 | Direct (4.92 h) | [39] |
| IRESEN (Under construction) | Morocco | LFC | 11400 | Mineral oil | 300/180 | Exergy Organic EPS 150 (solar only) | 1 | Buffer (20 min) | [40] |
| eCare Solar Thermal Plant (n.a.) | Morocco | LFC | 10000 | Water | 280/160 | n.a. | 1 | Steam Drum (2 h) | [41] |

As reported in Table 1, very few CSP-ORC power plants with a power output higher than 50 kW are currently operating in the world. On the other hand, solar ORC integrated with TES systems may have a role to play in meeting energy needs as a dispatchable power source in the future. The achievement of this goal requires the study and development of suitable operational strategies, able to produce electricity from solar energy following scheduled profiles and to provide ancillary services at distribution level.

In this framework, this paper focuses on the ongoing studies at the Ottana solar facility, a pilot power plant owned by ENAS (Ente Acque della Sardegna) in operation by September 2017 in Sardinia (Italy), based on a 630 kW CSP plant and a 400 kW Concentrating Photovoltaic (CPV) plant. After a detailed description of the main sections of the plant, with particular focus on the ORC unit, the novel operational strategy adopted for determining the ORC daily power profiles is introduced. It is based on a scheduling procedure, which defines one-day ahead the ORC power output profile in function of CSP state and weather forecast for the following day. Preliminary operating results and the expected performance of the CSP plant are finally presented and discussed.

## 2 The Ottana solar facility

The Ottana solar facility (Figure 1) is an experimental solar power plant with an overall power output of about 1 MW located in the industrial district of Ottana, Italy (40°14'18.9"N 8°59'37.7"E). The facility integrates a 630 kW CSP-ORC plant, including a thermal energy storage system, with a 400 kW CPV plant equipped with a molten-salt battery system. The electricity generation of the CSP and CPV sections will be primarily used for supplying the demand of the ENAS pumping stations. The Ottana pilot solar plant has also an experimental and demonstration purpose. In particular, the facility pursues the main goal of integrating effectively two different solar concentrating technologies and energy storage systems for enhancing the dispatch capabilities of solar power plants. In other words, the CSP+CPV plant does not only aim to maximize the energy production (as in typical commercial solar power plants) but also to study the ability of the integrated solar system to deliver scheduled profiles in accordance with the weather forecasting [39].

As shown in Figure 2, the CSP plant includes three main sections: the Solar Field (SF), where the solar energy is concentrated to heat up the HTF, a two-tank direct TES section, where the HTF is stored, and a Power Block (PB), where the collected thermal energy is converted into electricity. The Solar Field is composed of six lines of linear Fresnel collectors connected in parallel and aligned along the North-South direction. Each collector loop includes 34 modules for an overall length of 200 m and a net collecting area of 1432 $m^2$.

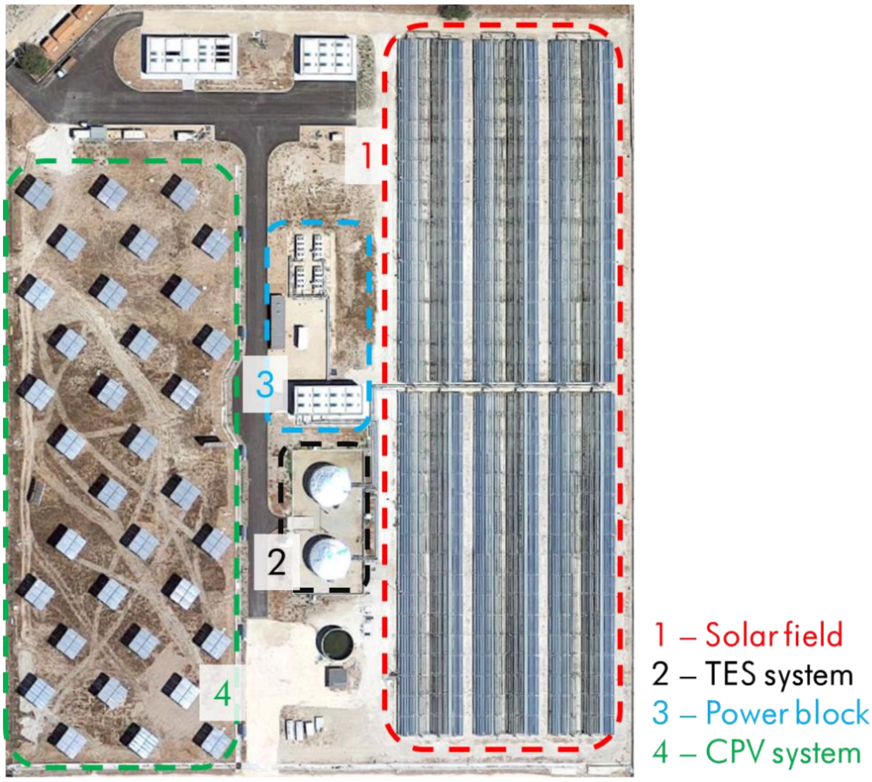


*Figure 1 – Aerial view of the Ottana solar facility.*

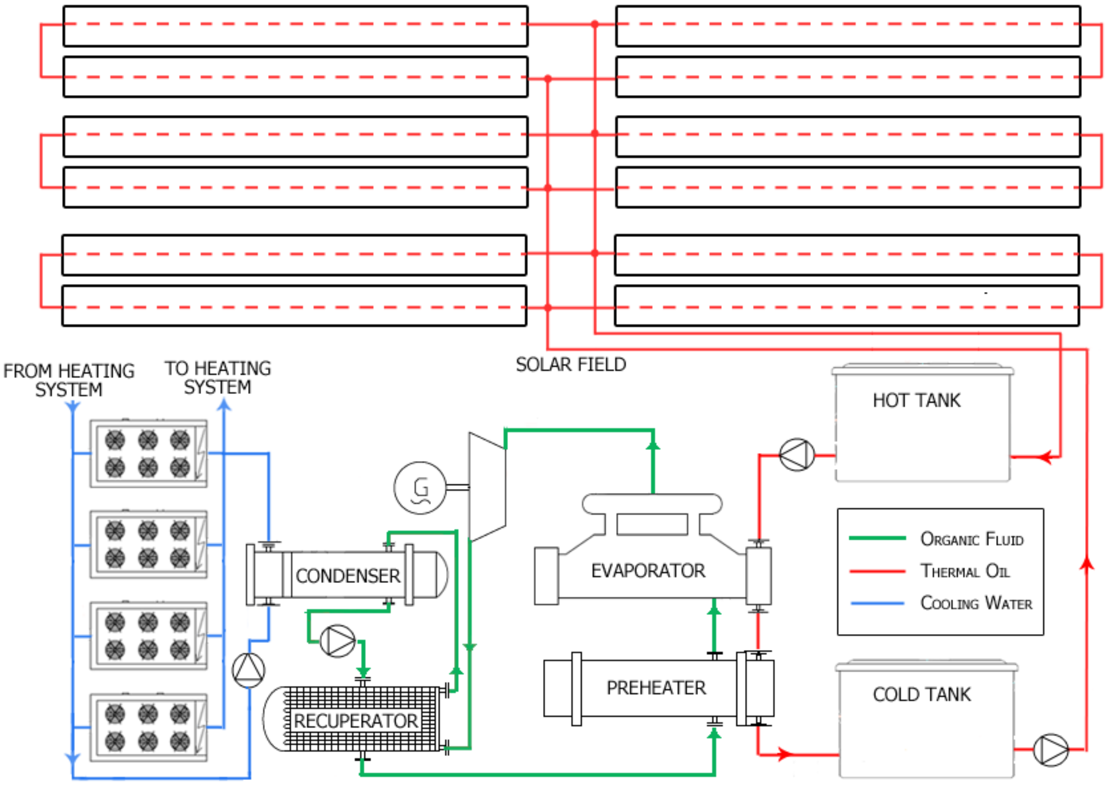


*Figure 2 - Schematic view of the CSP section of the Ottana solar facility.*

The primary mirrors (AGC Float type) concentrate the solar radiation onto the fixed receiver (7 m above the mirrors plane) that includes a secondary reflector and the evacuated receiver tube (Archimede HCEOI12 type). The heat transfer fluid is a commercial Therminol SP-I thermal oil, with a design inlet/outlet temperature of 165/275°C. Under nominal conditions (DNI of 900 $W/m^2$ , incident angle of 0°, ambient temperature of 20°C), the optical efficiency is 65.6%, which drops to 64.0% by considering also thermal losses in the receiver tube and piping. The thermal power produced by the solar field is about 5 MW, with a corresponding solar multiple of 1.6. The nominal HTF mass flow rate is 18 kg/s, while two circulating pumps controlled by a specific control system adjust its value under real conditions. The thermal energy storage section includes two storage tanks designed to store about 195 tonnes of thermal oil at a maximum temperature of 275°C. The capacity of the storage system is equal to 15.2 $MWh_t$, corresponding to 4.9 equivalent hours of the ORC operation at nominal conditions. The hot tank collects the thermal oil heated by the solar field and supplies it to the ORC unit; the cold tank receives the oil coming from the power block and supplies it to the solar field. Each tank includes a thermal insulation of mineral wool (walls), foam glass (bottom), calcium silicate (roof) and the upper volume of the storage tanks, above the oil, is filled with nitrogen to avoid oil oxidation.

The ORC unit is a Turboden 6HR Special, a 629 kW turbogenerator based on a regenerative Rankine cycle operated by an organic fluid (hexamethyldisiloxane, $C_6H_{18}OSi_2$). The latter is preheated and vaporized in an economizer (shell and tubes heat exchanger) and an evaporator (kettle reboiler type) respectively, both fed by the thermal oil from the hot tank. The working fluid is then sent to a 3-stage axial turbine (rotational speed of 3000 rpm) coupled with an electric generator (asynchronous type, air cooled), where the thermal energy is converted into electricity. Owing to the molecular complexity of the organic fluid, a small enthalpy drop occurs in the expansion phase, resulting in a large thermal power availability at the turbine discharge. To increase the cycle efficiency, a heat recovery unit (finned tubes heat exchanger) between the turbine and the condenser is introduced for a regenerative preheating. The exhaust working fluid is then sent to a water cooled condenser where it returns to saturated liquid conditions and, finally, it is pressurized in a multistage centrifugal feed pump coupled with an inverter controlled electric motor. The water from the condenser is cooled in turn by dry coolers and, in case, used for underfloor heating of control rooms and offices.

Besides the CSP section, the solar facility includes a CPV section coupled with an electrical energy storage system. This section is composed of 36 two-axis solar trackers, where six panels Soitec CX-M500 are arranged in each tracker. The optics are based on the Fresnel “silicon on glass” technology for a geometric concentration factor of 500 suns. Each panel is characterized by a nominal power of 1.985 $kW_p$ and a nominal efficiency of 29.8% under standard conditions. Owing to the high variability and poor predictability of the power produced by CPV modules, a battery bank FIAMM Spring based on Sodium–Nickel batteries is introduced for short-term energy storage (storage capacity of 430 kWh).

The facility includes a single connection point with the national grid and, therefore, the CSP and CPV sections are not completely independent of each other but they constitute a hybrid and integrated power plant. The hybridization of the CSP and CPV sections mainly occurs during the daily operation, where the different dynamic response of the two systems to DNI fluctuations (very fast for the CPV and relatively slow for the

CSP) allows to obtain an effective regulation of the scheduled profile. A support of the batteries to the ORC system even occurs during the start-up phases to cover the ORC ancillary consumptions. The structure of the control system is based on a three-level hierarchical model: the first level is related to a scheduling procedure for the determination of the one-day ahead CSP+CPV power profile, a real-time control algorithm is implemented in the second level for the power profile tracking according to actual meteorological data and the last level involves the control systems of each component of the plant.

## *2.1 ORC performance*

As mentioned, the Turboden 6HR Special is designed to produce a net electrical power of 629 kW with a net efficiency of 20.3% under nominal conditions. Table 2 reports the ORC unit performance at reference conditions, but the ORC often works far from nominal conditions, as confirmed by the first experimental results.

Depending on the operational strategy, the ORC unit can operate at part-load conditions and the control system meets this requirement by reducing the oil mass flow rate with a consequent decrease of the organic fluid mass flow rate circulated by the pump. During high partial loads, the turbine adapts to the actual flow conditions with a decrease of the input pressure (sliding-pressure control) and a consequent decrease of the enthalpy drop. However, a combination of sliding pressure and throttling is applied at low partial loads to avoid premature evaporation of the organic fluid in the regenerator. Obviously, the use of the sole sliding pressure control leads to a lower decrease of the isentropic efficiency of the expander.

*Table 2 - ORC performance at reference conditions.*

| | |
|---|---|
| **INPUT – Thermal oil** | |
| Thermal oil inlet temperature | 275°C |
| Thermal oil outlet temperature | 165°C |
| Thermal oil mass flow rate | 11.05 kg/s |
| Thermal power input | 3100 $kW_t$ |
| **OUTPUT – Cooling water** | |
| Cooling water inlet temperature | 25°C |
| Cooling water outlet temperature | 35°C |
| Thermal power to condenser | 2436 $kW_t$ |
| **PERFORMANCE** | |
| Gross electrical power | 664 kW |
| Gross electrical efficiency | 21.4% |
| Captive power consumption | 35 kW |
| Net electrical power | 629 kW |
| Net electrical efficiency | 20.3% |
| Electric generator | 50Hz/400 V |

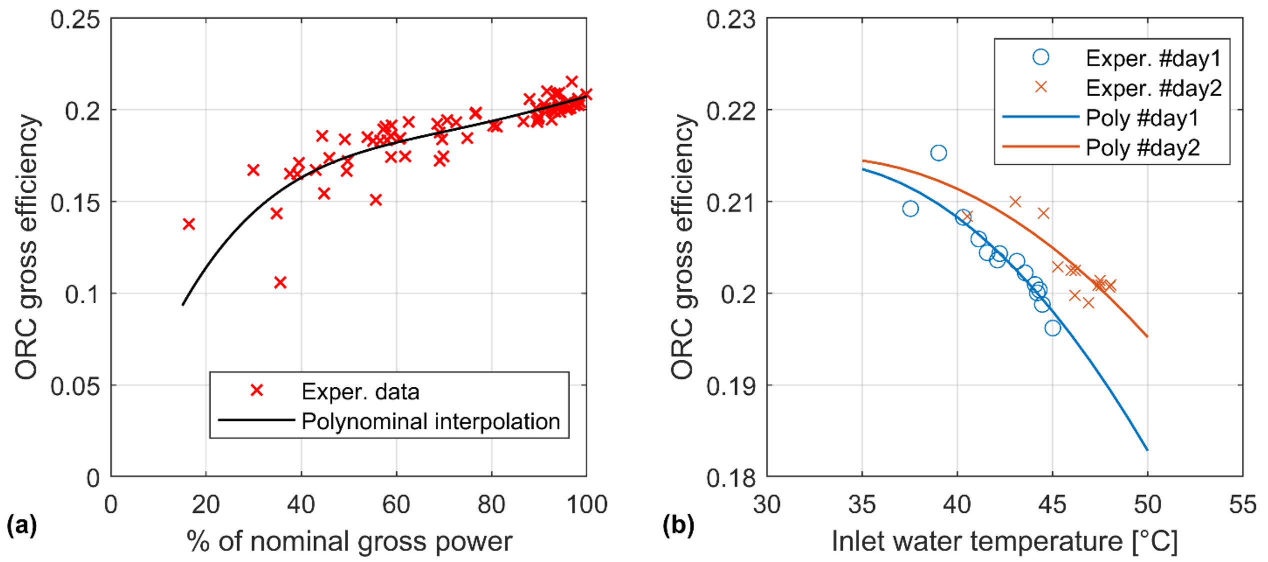


*Figure 3 – (a) ORC performance at part-load conditions and (b) Effect of the water temperature at the condenser inlet side on the ORC gross efficiency.*

This fact is highlighted in Figure 3(a), where is depicted the ORC efficiency at part-load conditions: the degradation of the ORC performance from 100% up to 50% of the nominal gross power is lower than 3 percentage points, while the performance drop becomes more evident with part-load conditions lower than 40%. In Figure 3(a), experimental data measured during the first operating period of the CSP plant are also reported. The high dispersion of experimental data is mainly due to different conditions in terms of ambient temperature and thermal oil inlet temperature. As mentioned, the condenser waste heat is removed by dry coolers. Consequently, the water temperature at the condenser inlet side depends on the ambient temperature. Obviously, an increase of the inlet water temperature leads to an increase of the minimum pressure of the ORC thermodynamic cycle with a consequent degradation of the cycle efficiency. Conversely, a decrease in the maximum cycle pressure compared to the nominal one occurs with the decrease of the thermal oil inlet temperature due to the hot tank heat losses. Figure 3(b) shows the influence of the inlet water temperature and inlet thermal oil temperature on the ORC performance during two different operating days. During these days, an increase of the water temperature at the condenser inlet side has been detected due to a rise in the ambient temperature along the day (about 7°C for both days). On the other hand, a different thermal oil inlet temperature has been measured (about 15°C on average), causing a different trend of the ORC gross efficiency between the two days. Finally, an important feature of the solar-ORC system is the unavoidable daily start-up and shut-down phases of the ORC turbogenerator due to the limited solar energy availability. To allow a fast start-up time during the following day, the organic fluid and the hot components are kept in temperature during the shut-down phase by a minimal thermal oil mass flow that continuously feeds the ORC unit. Figure 4 shows the main energy flows measured during a test-day, highlighting the thermal power input required during the so-called hot start-up. This phase has a duration of 50 minutes with a thermal energy consumption of about 550 $kWh_t$. On the other hand, an ORC stop longer than one day may occur during some periods of the year, especially in winter and mid-season. In this case, the feeding of a minimal thermal power input during the shut-down phase can be stopped. A longer ORC start-up (the so-called cold start-up) occurs and higher amount of energy for warming up the metallic parts of the turbogenerator and for vaporizing the working fluid is required.

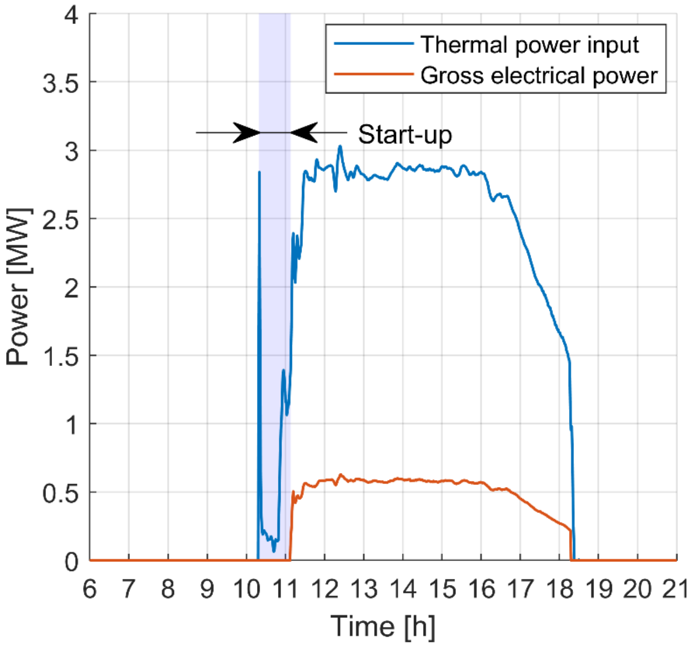


*Figure 4 – Thermal power input and gross electrical power of the ORC unit during an operative day, with evidence of the energy flows during the start-up phase.*

## 3 Operational strategy: determination of the daily power profile

As mentioned, the operational strategy adopted for the CSP plant is based on an optimal scheduling procedure that determines the daily power profile one-day ahead by taking into account forecasted CSP+CPV power production profile, storages status and availability. The development of a novel and integrated control logic is therefore required for the definition of the set-point of the CSP+CPV power production for the following day. In particular, the control strategy adopted for the ORC unit has a dual purpose. The first objective aims at maximizing the energy production, promoting the use of the ORC unit close to design conditions with a starting time scheduled after the complete filling of the hot tank (similar to the control strategy of the large-size CSP plants in operation today). The second objective pursues the hybridization of the two solar systems, that is, ensuring the matching between CPV and ORC power delivery periods both to exploit the CSP peculiarities of "semi-dispatchability" and to minimize the fluctuations in the production of CPV. Unlike the previous scope, the operation at part load conditions is often required in this case, especially during partly cloudy days.

The algorithm proposed for the definition of daily ORC profiles determines the best trade-off between this two conflicting goals by considering the expected energy production and fluctuations for the following day.

In particular, two main inputs are required: the plant status at the end of the previous day and the weather forecast data delivered by a specific service. In particular, the expected DNI and the ambient temperature

($T_{AMB}$) are used for calculating of the expected solar field energy production ($\widetilde{E}_{SF}$). The latter is evaluated by using the simulation model presented in [42] and can be summarized by the following relationship:

$$\widetilde{E}_{SF} = \sum_{t=1}^{24} \left[ \widetilde{DNI}(t) \cdot A_{SF} \cdot \eta_{OPT}(t) - \dot{Q}_{L,TH}(\widetilde{T}_{AMB}(t)) \right] \tag{1}$$

where $A_{SF}$ is the solar field collecting area, $\eta_{OPT}$ is the optical efficiency and $\dot{Q}_{L,TH}$ are the thermal losses in the receiver tubes and piping calculated as a function of the ambient temperature. The tilde sign is added to the parameters based on forecast data, which are subjected to uncertainty. The storage status is described in terms of average oil temperature $T_{HT}$ and stored oil mass $M_{HT}$ and is represented by the Filling Level ($FL_{HT}$), which is defined as the ratio between the current $M_{HT}$ and the maximum mass storable in the hot tank $M_{HT,MAX}$. The stored energy in the hot tank ($E_{HT}$) is therefore calculated as:

$$E_{HT} = (FL_{HT} - FL_{MIN}) \cdot M_{HT,MAX} \cdot c_{HTF} \cdot (T_{HT} - T_{CT,NOM}) \tag{2}$$

where $c_{HTF}$ is the specific heat of the thermal oil, $T_{CT,NOM}$ is the nominal cold tank temperature (165°C) and $FL_{MIN}$ is the minimum filling level. The latter is a control parameter introduced to ensure a minimum amount of HTF inside the hot tank suitable to cover fluctuations in thermal energy production and eventual overestimations of expected solar field energy production. Therefore, the overall thermal energy input $\widetilde{E}_{IN}$ available for the ORC unit for the following day is the sum of the stored energy already available in the hot tank and the expected daily energy production of the solar field:

$$\widetilde{E}_{IN} = E_{HT} + \widetilde{E}_{SF} \tag{3}$$

The main output of the control algorithm is the ORC delivery profile for the following day, simply evaluated by assuming a constant ORC power output. As shown in Figure 5, four parameters are required to define this profile: the ORC on/off state, the net electrical power output $P_{EL}$, the corresponding duration period $\tau_{ORC}$ and the start-up time $t_{ON}$.

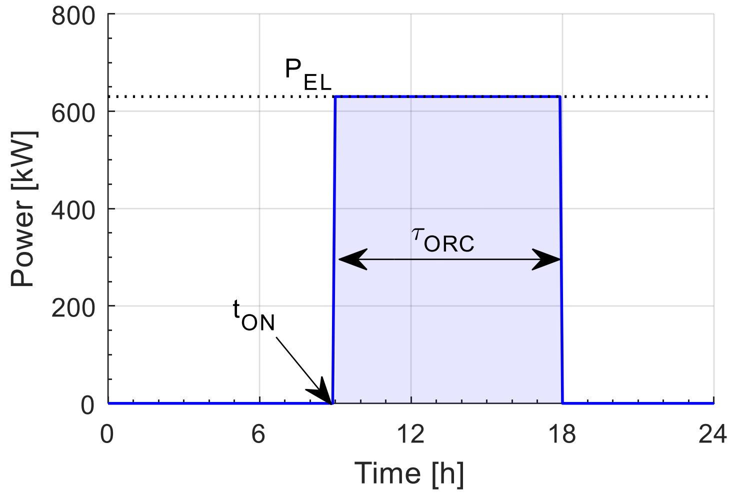


*Figure 5 – Example of a daily power output determined by the adopted control strategy.*

An index K is introduced as the main control parameter that determines the trade-off between the two objectives. It is defined as the ratio between the expected solar field energy production $\widetilde{E}_{SF}$ and the corresponding solar field energy production in clear-sky conditions $E_{SF,MAX}$. The expected K index for the following day determines the priority assigned to the optimization of ORC performance or to the matching between CPV and ORC power delivery periods, through the introduction of two threshold values ($K_{HIGH}$ and $K_{LOW}$). High K values ($K>K_{HIGH}$) result from stable atmospheric conditions and marginal fluctuations on the CPV power production, limiting the role of the CSP section in the supporting of CPV production. In these cases, the maximization of the ORC performance is preferred and the ORC state is set to ON-FULL. The electrical power output is calculated in function of the expected average oil temperature in the hot tank and of the foreseen maximum ambient temperature for the following day, by assuming a thermal oil mass flow rate at nominal conditions. Accordingly, the duration period is evaluated by considering the expected thermal energy availability $\widetilde{E}_{IN}$ and the calculated $P_{EL}$. Vice versa, since low K values ($K< K_{LOW}$) result in very low solar energy availability, the ORC unit is kept off (state OFF) and the eventual solar field energy production is stored in the hot tank. For intermediate values of K ($K_{LOW}<K<K_{HIGH}$), the decision about the on/off state of the ORC unit strongly depends on $\widetilde{E}_{IN}$ (in particular on the energy stored $E_{HT}$ in the hot tank at the end of the previous day). If the expected $\widetilde{E}_{IN}$ is not sufficient to guarantee a minimum number of operating hours $\tau_{ORC,MIN}$ at nominal conditions (here imposed equal to 2 hours) the ORC unit is kept off, otherwise the start-up of the ORC unit is scheduled. In this case, the support of the ORC unit to the CPV power production becomes fundamental and, in order to ensure the operation of the ORC during the production period of the CPV system, $\tau_{ORC}$ is set equal to the CPV delivery period ($\tau_{CPV}$). The ORC state is set to ON-PART and the ORC power level is subsequently calculated according to the overall energy availability and the imposed duration period. However, to avoid a drop in the ORC performance, a constraint in the minimum ORC power output ($P_{EL,MIN}$) is introduced and set to 50% of the nominal power. In the latter case, the ORC state is set to ON-MIN and the delivery period $\tau_{ORC}$ is adjusted in order to satisfy this constraint.

Finally, the start-up time $t_{ON}$ is determined based on the energy stored in the hot tank. As said, a minimum filling level ($FL_{MIN}$) is required to guarantee the oil supply during the start-up phase, as well as to absorb the fluctuations in the thermal energy production during the day. If the $FL_{HT}$ at the end of the previous day is lower than $FL_{MIN}$, the ORC start up is postponed until a safe level of stored energy is achieved with the solar field energy production in the first sunshine hours. Otherwise, $t_{ON}$ is set equal to the first hour of the day where a share of solar field production is expected. The flowchart of the procedure for the determination of the ORC delivery profile is shown in Figure 6.

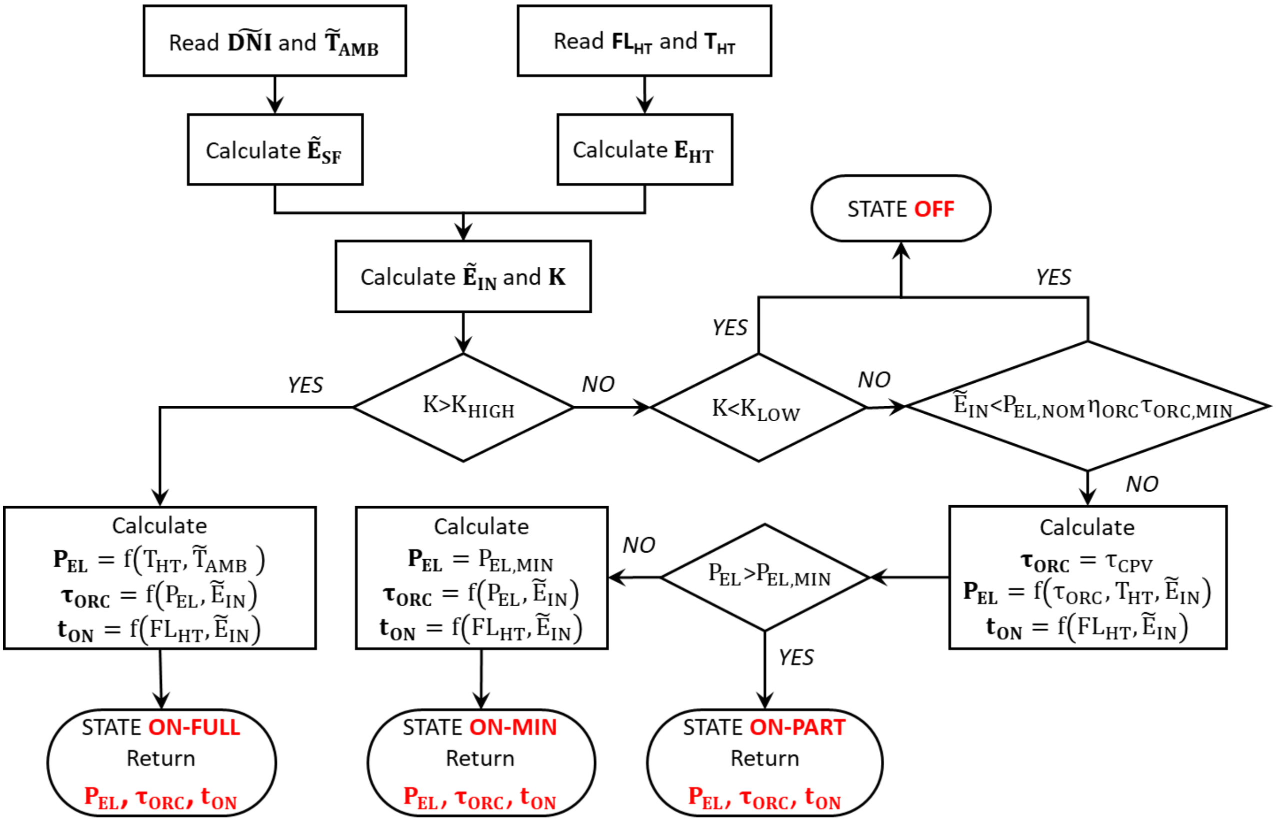


*Figure 6 – Operational strategy for scheduling the ORC daily power profile.*

## 4 Results and discussion

The expected performances of the CSP section of the Ottana solar facility are presented and analysed in this section. The operational strategy presented in the previous section and based on weather forecast data is used for the determination of the day-ahead power generation profile of the ORC unit. The latter and the actual weather conditions are then used as main inputs for simulating the actual daily operation of the CSP section. A dedicated simulation model developed in Matlab is used for evaluating the actual thermal power production of the solar filed $\dot{Q}_{SF}$ and the corresponding thermal oil mass flow rate [42]. On the other hand, the thermal power input $\dot{Q}_{PB}$ and the corresponding mass flow rate required by the power block are calculated according to the ORC scheduled profile, the actual water inlet temperature and the current oil temperature in the hot tank. The oil mass stored in the hot tank $M_{HT}$ is therefore used to compensate the mismatch between the thermal energy produced by the SF and that required by the ORC unit. If the hot tank is fully charged, some mirrors are defocused to maintain the thermal power balance. This originates an excess power neither used nor stored, which leads to the so-called defocusing power losses $\dot{Q}_{DEF}$. Conversely, if the hot tank is completely empty and the mass flow rate produced by the solar is lower than that required by the ORC unit, the actual ORC power output is reduced compared to the scheduled one or the turbogenerator is shut down if the SF mass flow rate is unable to guarantee the minimum part-load ratio. This lack of energy production compared to the scheduled one results in a share of undelivered power.

In this section, the ability of the solar ORC plant to follow scheduled profiles, the effect of the uncertainty in weather forecast and the influence of the main control parameters on the ORC state and efficiency are investigated. The forecast data provided by a weather forecast service and the measured data of the main meteorological parameters are used. Firstly, the plant performance during a typical daily operation is presented. The analysis is then extended to a yearly basis for the evaluation of the expected annual performance.

### *4.1 Daily performance*

The weather conditions occurring in Ottana on 19/05/2017 (a day of testing during commissioning) are selected as case study. Figure 7 shows the expected and measured values of the DNI and ambient temperature. The uncertainty on expected DNI trend is highlighted in Figure 7(a), since the weather forecast service overestimates the daily DNI (6.71 kWh/m$^2$ instead of 6.24 kWh/m$^2$ actually measured on the daily basis). In addition, the forecast trend is unable to detect the high fluctuations on the beam solar radiation. A deviation in the ambient temperature trend is also observed during the considered day (Figure 7(b)). In particular, a mean difference of +5°C is detected between measured and expected values. This deviation leads to a wrong estimation of both the water temperature at the condenser inlet side and the thermal losses of the receiver tube (although the influence on this parameter is marginal). The effect of the weather forecast uncertainty on the solar field energy production is shown in Figure 8(a). The overestimation of the solar energy availability leads to a difference between the expected SF thermal energy production ($\widetilde{E}_{SF}$) and the actual one ($E_{SF}$) of 0.4 MWh$_t$, although a maximum difference of 2.1 MWh$_t$ in the cumulative SF production is observed during the day. Starting from a stored oil mass in the hot tank ($FL_{HT}$) equal to the minimum allowed value ($FL_{MIN}$ set equal to 20% of the overall capacity), the expected K value is equal to 0.69. Since this is an intermediate value between $K_{HIGH}$ (imposed equal to 0.8) and $K_{LOW}$ (set equal to 0.2), the operational strategy ON-PART is by the proposed control strategy. The ORC delivery profile is characterized by a net power output of 330 kW, a duration time of 12 h and a start-up time established at 9 a.m. The corresponding thermal power input ($\dot{Q}_{PB}$) including start-up thermal demand is shown in Figure 8(b), together with the thermal power produced by the solar field ($\dot{Q}_{SF}$) and the evolution of the hot tank filling level ($FL_{HT}$). It is worth noting the important role of the TES system for compensating both the fluctuations on the SF thermal energy production and the uncertainty in weather forecast. Although the scheduled power output profile was set to achieve no difference between the initial and final filling level of the hot tank, the oil mass stored into the hot tank at the end of the day is equal to 11.9% of the overall capacity (instead of 20%). This mismatch is mainly due to the expected and actual SF energy production and the higher ORC thermal power input. Consequently, the SF energy production of the following day is required to restore the minimum filling level of the hot tank and the start-up time is postponed until the minimum $FL_{HT}$ is reached.

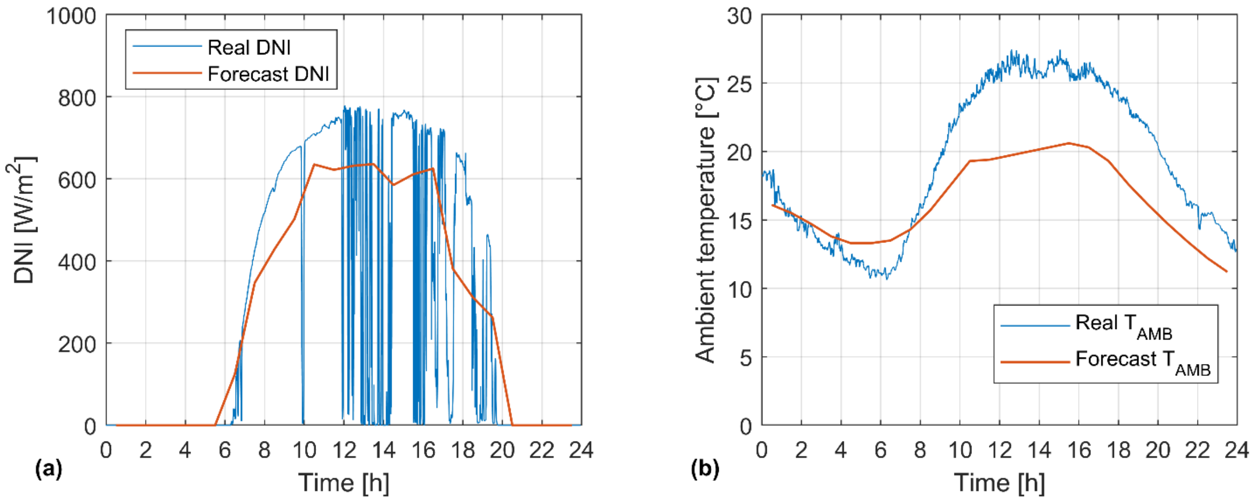


*Figure 7 – Comparison between the forecasted and real weather data occurring in Ottana on 19/05/2017 in terms of (a) Direct Normal Irradiance and (b) ambient temperature.*

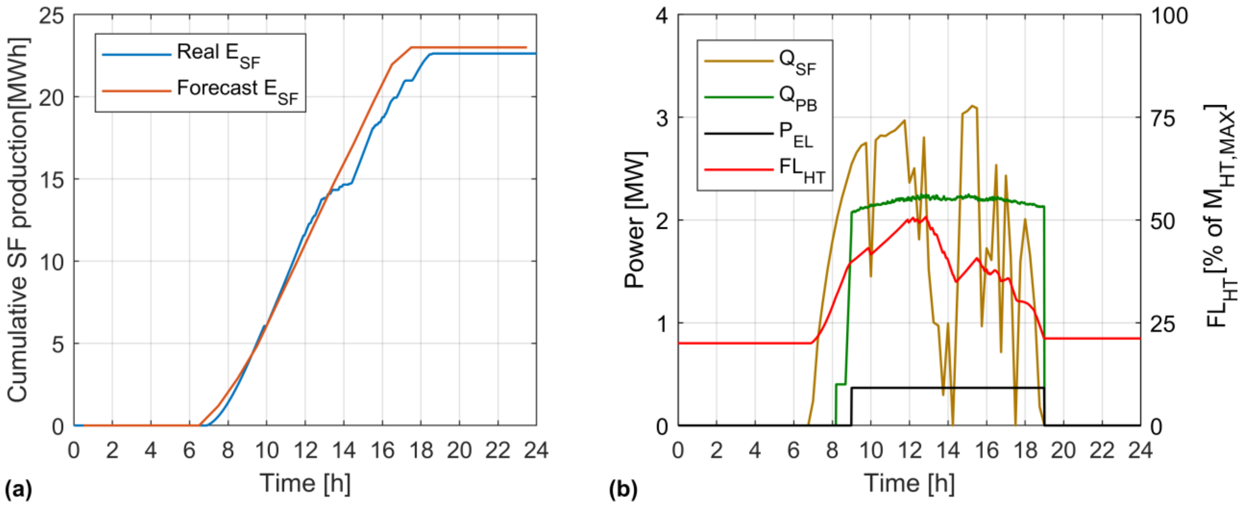


*Figure 8 – (a) Comparison between expected and real cumulative solar field production and (b) main energy flows*

### *4.2 Annual performance*

In this section, the proposed operational strategy is tested in a yearly-based analysis, with the aim of assessing the expected performance and evaluating the effect of the main control parameters. Because of the unavailability of annual meteorological data for the Ottana site, weather forecast data and real weather data referred to Rome (Italy) are used in this analysis, as if the plant was located in the Rome area. On the other hand, because of the two locations (Ottana and Roma) have similar latitude (40°14’ for Ottana and 41°53’ for

Rome), no important variations on the annual meteorological conditions and, thus, on the main plant performance should occur. The annual solar energy availability for the considered site is about 15 GWh. However, due to the optical and thermal losses, the annual SF energy production is about 4.75 GWh (the eventual defocusing losses are not considered here), resulting in an average efficiency of about 32%. As mentioned, the definition of the daily power output profile depends on the expected solar field energy production, which usually differs from the actual one due to weather forecast uncertainty. Figure 9 shows the difference between the expected daily SF energy production and the real one detected during the period analysed. A mean absolute deviation of 2.9 $MWh_t$/day is found and the weather forecast often underestimates the actual solar energy availability (the mean bias error is -1.9 $MWh_t$).

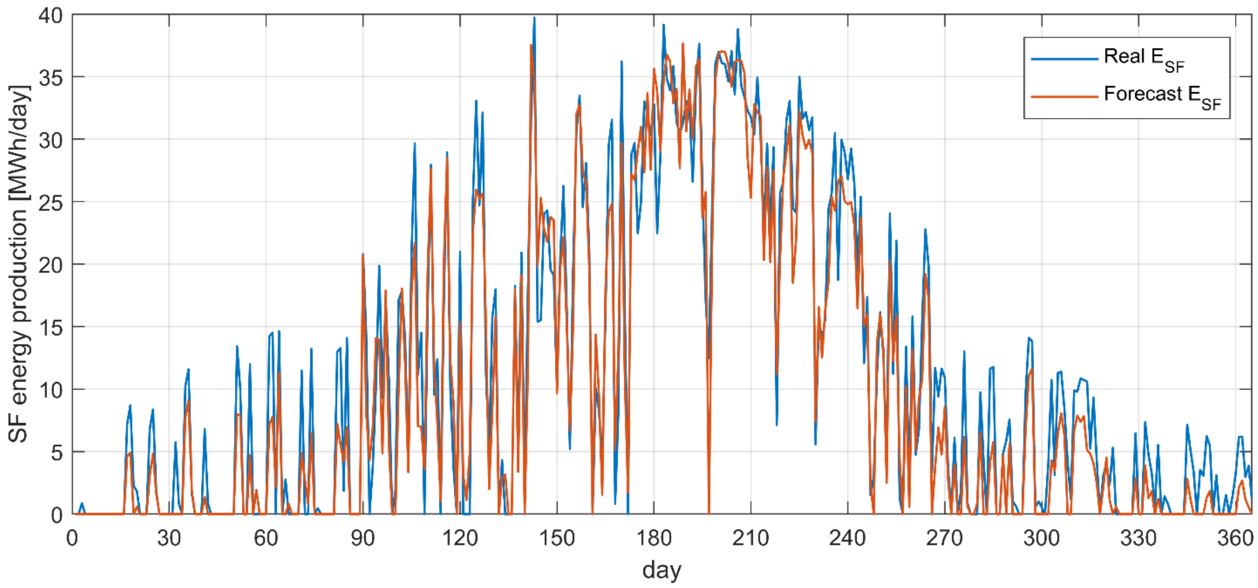


*Figure 9 – Annual trend of the expected and real daily SF energy production.*

This leads to the risk of a complete filling of the hot tank and the subsequent defocusing of the solar field or a complete emptying of the hot tank and the consequent non-fulfilment of the power output profile. For this reason, the adoption of a suitable operational strategy for the management of the energy flows from/to the TES system becomes fundamental. The effect of weather forecast inaccuracy on the main plant performances is reported in Table 3, where the main results obtained by the weather forecast case (use of weather forecast data) are compared with those obtained by the ideal case, in which weather forecast data and real data coincide. In both cases, the main control parameters are set as $K_{LOW}$=0.2, $K_{HIGH}$=0.8 and $FL_{MIN}$=0.2. The underestimation of the SF energy production by using weather forecast leads a decrease of the operating days and a rise in the annual defocusing losses compared to those obtained in the ideal case. Consequently, a reduction of about 7% of the annual electricity production is expected for the weather forecast case with respect to that obtained for the ideal one.

*Table 3 – Effect of weather forecast inaccuracy on the main plant performance*

| | **Weather forecast case** | **Ideal case** |
|---|---|---|
| Average electrical power output [MW] | 413 | 411 |
| Delivery duration period [h] | 8.37 | 7.11 |
| Number of operating days | 212 | 254 |
| Annual electricity production [GWh/y] | 0.731 | 0.784 |
| Defocusing losses [GWh/y] | 0.269 | 0 |
| Undelivered electrical energy [GWh/y] | 0.06 | 0.05 |

As already mentioned, the operational strategy proposed uses three threshold values that largely influence the performance of the system: $K_{LOW}$, which determines the off state of the ORC unit during cloudy days, $K_{HIGH}$, which sets the working point of the ORC unit and $FL_{MIN}$, which represents the minimum HTF level in the hot tank for a safe start-up. For this reason, starting from the previous weather forecast case where $K_{LOW}$=0.2, $K_{HIGH}$=0.8 and $FL_{MIN}$=0.2, the influence of each parameter on the annual performance of the plant has been evaluated. The effect of $K_{LOW}$ on the performance of the CSP section is shown in Figure 10. In particular, the influence of $K_{LOW}$ on the ORC operating states during the annual simulation are depicted in Figure 10(a). This figure proves a decrease of the number of ORC start-ups and a reduction in the ORC operating hours at minimum load with the increase of $K_{LOW}$. Consequently, as shown by Figure 10(b), a rise in $K_{LOW}$ results in a daily power profile characterized by higher values of both the average electrical power output and delivery duration and therefore an increment in the average ORC efficiency. As shown by Figure 10(c), the effect on the annual performance is the reduction of the annual electricity production ($E_{EL}$) due to the decrease of the thermal power input required by the PB, the consequent increase of the annual defocusing thermal losses ($E_{DEF}$), and the reduction in the overall undelivered electrical energy ($E_{UN}$).

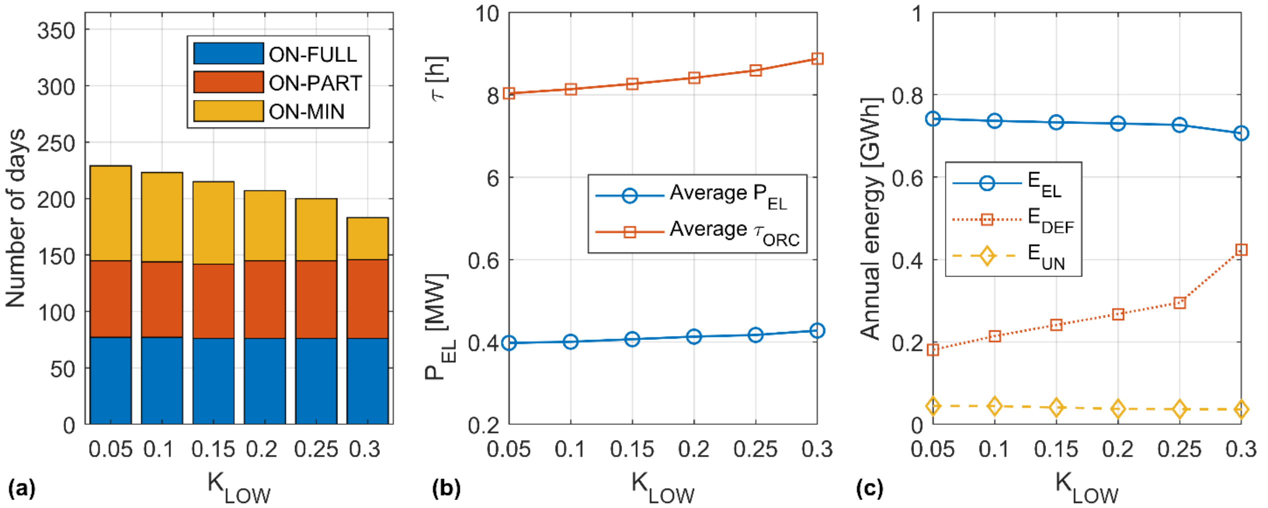


*Figure 10 - Influence of the $K_{LOW}$ on (a) the ORC state, (b) the average electrical power output and delivery duration period, (c) annual electricity production, defocusing losses and undelivered energy.*

Another important parameter is the minimum filling level of the hot tank. As demonstrated by Figure 11, the effect of this control parameter on the ORC state is marginal and the number of ORC start-up is almost constant. On the other hand, the daily start-up time is often postponed to guarantee a safe start-up and even the stored energy in the hot tank available for the scheduling procedure is reduced. In other words, the rise in the $FL_{MIN}$ favours a more conservative approach with a lower average delivery duration period (the average electrical power output remains almost constants). Consequently, a reduction of the annual electricity production is observed, with a lower requirement of the ORC thermal power input and the rise in the occurrence of full charge states of the hot tank and the defocusing of the solar field. At the same time, an important reduction of the undelivered power is observed, since the eventual overestimation of the available thermal energy for the following day is completely covered by the energy stored in the hot tank.

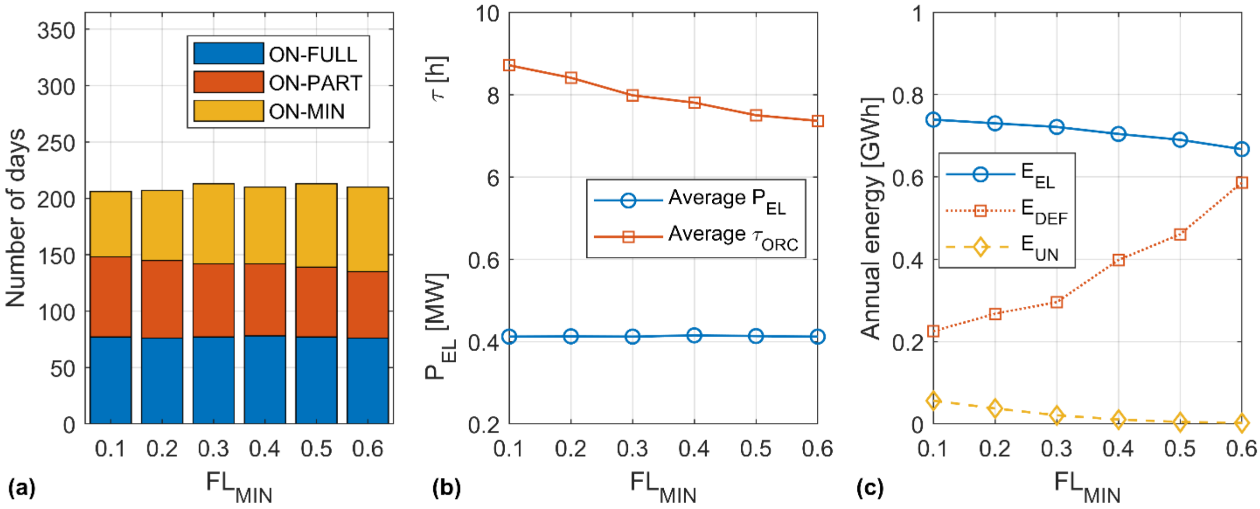


*Figure 11 - Influence of the $FL_{MIN}$ on (a) the ORC state, (b) the average electrical power output and delivery duration period, (c) annual electricity production, defocusing losses and undelivered energy.*

Finally, the influence of the $K_{HIGH}$ control parameter on the main expected performance of the CSP section is shown in Figure 12. Since this parameter is not involved in the determination of the ORC state during days characterized by low K values, the number of annual ORC start-up and percentage of occurrence of ON-MIN states remain almost constant. On the other hand, low values of this parameter increase the percentage of occurrence of ORC operating states at full load conditions. However, the effect on the ORC performance is rather marginal both in shape of the ORC power profile and annual energy performance.

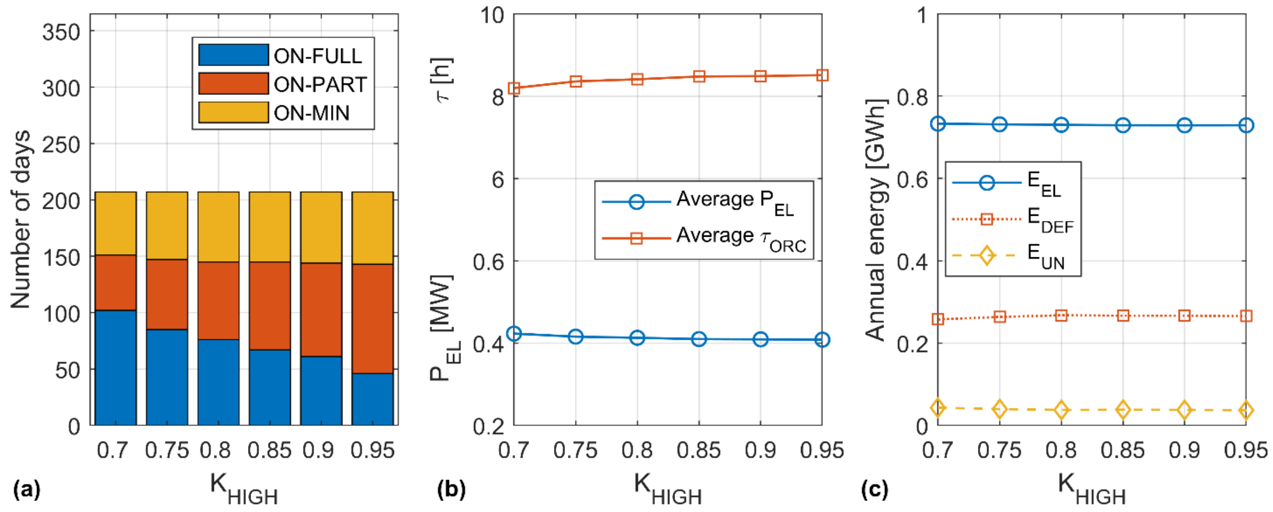


*Figure 12 - Influence of the $K_{HIGH}$ on (a) the ORC state, (b) the average electrical power output and delivery duration period, (c) annual electricity production, defocusing losses and undelivered energy.*

## 5 Conclusions

This paper reported the first operating results and the expected annual performance of the CSP-ORC plant at the Ottana solar facility, a new experimental power plant located in Sardinia (Italy).

The first operating results demonstrated that the ORC performance significantly depend on the thermal oil inlet temperature and on the ambient temperature. In particular, due to the use of dry coolers, the increase of the ambient temperature leads to a corresponding increase of the condensing temperature of the working fluid with a corresponding reduction of the ORC cycle efficiency. Moreover, the first operating data highlighted the important role of the daily start-up and shut-down phases of the ORC unit. The latter are of minor importance in conventional ORC applications (biomass, geothermal, etc.), but in case of solar energy as unique heat source, the daily start-up and shut-down phases require the development of a suitable management strategy in order to minimize the corresponding thermal energy requirements.

The integration of a CSP plant with a CPV system, with the aim of producing dispatchable power from solar energy requires the development of a proper control strategy able to define the daily power profile for the following day starting from weather forecasting data. The analysis of the expected performance of the CSP plant carried out in the paper demonstrated that the average ORC efficiency, the annual electrical production and the ability of the plant to follow scheduled power profile minimizing the undelivered energy remarkably depend on the control parameters assumed to set the on/off status of the ORC plant. Finally, it is worth noting that the effort in offering dispatchable electrical power from a not-programmable source (solar energy) is not currently recognized in monetary terms, despite the important advantages for the grid operator arising from the application of these scheduling procedures. On the other hand, the introduction of future government incentives for energy dispatchability from non-programmable renewable sources will be required to enhance the RES penetration into the grid.

## 6 Acknowledgements

The Ottana solar facility is founded by the Regional Government of Sardinia (Italy) in the framework of the operational program ERDF 2007-2013. The institutional supervisor of the project is the Industry and Energy Office of Sardinian Regional government. The design and the building of the plant were entrusted to ENAS, the Sardinian Water Company. Sardegna Ricerche and the University of Cagliari are developing the research activities on the facility. ENAS will be in charge of the operation and management of the pilot plant.

## 7 References

[1] International Energy Agency. World Energy Outlook 2016. IEA Publications; 2016.

[2] Hernández-Moro J, Martínez-Duart JM. Analytical model for solar PV and CSP electricity costs: Present LCOE values and their future evolution. Renew Sustain Energy Rev 2013;20:119–32. doi:10.1016/j.rser.2012.11.082.

[3] González-Roubaud E, Pérez-Osorio D, Prieto C. Review of commercial thermal energy storage in concentrated solar power plants: Steam vs. molten salts. Renew Sustain Energy Rev 2017;80:133–48. doi:10.1016/j.rser.2017.05.084.

[4] Wagner SJ, Rubin ES. Economic implications of thermal energy storage for concentrated solar thermal power. Renew Energy 2014;61:81–95. doi:10.1016/j.renene.2012.08.013.

[5] Stekli J, Irwin L, Pitchumani R. Technical Challenges and Opportunities for Concentrating Solar Power With Thermal Energy Storage. J Therm Sci Eng Appl 2013;5:21011. doi:10.1115/1.4024143.

[6] Liu M, Steven Tay NH, Bell S, Belusko M, Jacob R, Will G, et al. Review on concentrating solar power plants and new developments in high temperature thermal energy storage technologies. Renew Sustain Energy Rev 2016;53:1411–32. doi:10.1016/j.rser.2015.09.026.

[7] Pietzcker RC, Stetter D, Manger S, Luderer G. Using the sun to decarbonize the power sector: The economic potential of photovoltaics and concentrating solar power. Appl Energy 2014;135:704–20. doi:10.1016/j.apenergy.2014.08.011.

[8] Dowling AW, Zheng T, Zavala VM. Economic assessment of concentrated solar power technologies: A review. Renew Sustain Energy Rev 2017;72:1019–32. doi:10.1016/j.rser.2017.01.006.

[9] Pelay U, Luo L, Fan Y, Stitou D, Rood M. Thermal energy storage systems for concentrated solar power plants. Renew Sustain Energy Rev 2017;79:82–100. doi:10.1016/j.rser.2017.03.139.

[10] Macchi E, Astolfi M. Organic Rankine Cycle Power Systems. 2017.

[11] Markides CN. Low-Concentration Solar-Power Systems Based on Organic Rankine Cycles for Distributed-Scale Applications: Overview and Further Developments. Front Energy Res 2015;3:47. doi:10.3389/fenrg.2015.00047.

[12] Aboelwafa O, Fateen S-EK, Soliman A, Ismail IM. A review on solar Rankine cycles: Working fluids, applications, and cycle modifications. Renew Sustain Energy Rev 2018;82:868–85. doi:10.1016/j.rser.2017.09.097.

[13] Desai NB, Bandyopadhyay S. Thermo-economic analysis and selection of working fluid for solar

organic Rankine cycle. Appl Therm Eng 2016;95:471–81. doi:10.1016/j.applthermaleng.2015.11.018.

[14] Rayegan R, Tao YX. A procedure to select working fluids for Solar Organic Rankine Cycles (ORCs). Renew Energy 2011;36:659–70. doi:10.1016/j.renene.2010.07.010.

[15] Bellos E, Tzivanidis C. Parametric analysis and optimization of an Organic Rankine Cycle with nanofluid based solar parabolic trough collectors 2017. doi:10.1016/j.renene.2017.06.055.

[16] Tzivanidis C, Bellos E, Antonopoulos KA. Energetic and financial investigation of a stand-alone solar-thermal Organic Rankine Cycle power plant. Energy Convers Manag 2016;126:421–33. doi:10.1016/j.enconman.2016.08.033.

[17] Hajabdollahi H, Ganjehkaviri A, Nazri M, Jaafar M. Thermo-economic optimization of RSORC (regenerative solar organic Rankine cycle) considering hourly analysis. Energy 2015;87:369–80. doi:10.1016/j.energy.2015.04.113.

[18] Borunda M, Jaramillo OA, Dorantes R, Reyes A. Organic Rankine Cycle coupling with a Parabolic Trough Solar Power Plant for cogeneration and industrial processes. Renew Energy 2016;86:651–63. doi:10.1016/j.renene.2015.08.041.

[19] Chacartegui R, Vigna L, Becerra JA, Verda V. Analysis of two heat storage integrations for an Organic Rankine Cycle Parabolic trough solar power plant. Energy Convers Manag 2016;125:353–67.

[20] He Y-L, Mei D-H, Tao W-Q, Yang W-W, Liu H-L. Simulation of the parabolic trough solar energy generation system with Organic Rankine Cycle. Appl Energy 2012;97:630–41. doi:10.1016/j.apenergy.2012.02.047.

[21] Manente G, Toffolo A, Lazzaretto A, Paci M. An Organic Rankine Cycle off-design model for the search of the optimal control strategy. Energy 2013;58:97–106. doi:10.1016/j.energy.2012.12.035.

[22] Wang J, Yan Z, Zhao P, Dai Y, Woodruff GW. Off-design performance analysis of a solar-powered organic Rankine cycle. Energy Convers Manag 2014;80:150–7. doi:10.1016/j.enconman.2014.01.032.

[23] Calise F, Capuozzo C, Carotenuto A, Vanoli L. Thermoeconomic analysis and off-design performance of an organic Rankine cycle powered by medium-temperature heat sources. Sol Energy 2014;103:595–609. doi:10.1016/j.solener.2013.09.031.

[24] Hu D, Zheng Y, Wu Y, Li S, Dai Y. Off-design performance comparison of an organic Rankine cycle under different control strategies. Appl Energy 2015;156:268–79. doi:10.1016/j.apenergy.2015.07.029.

[25] Emi Dickes R, Dumont O, Emi Daccord R, Quoilin S, Lemort V. Modelling of organic Rankine cycle power systems in off-design conditions: An experimentally-validated comparative study 2017. doi:10.1016/j.energy.2017.01.130.

[26] Quoilin S, Aumann R, Grill A, Schuster A, Lemort V, Spliethoff H. Dynamic modeling and optimal control strategy of waste heat recovery Organic Rankine Cycles. Appl Energy 2011;88:2183–90. doi:10.1016/j.apenergy.2011.01.015.

[27] Freeman J, Guarracino I, Kalogirou SA, Markides CN. A small-scale solar organic Rankine cycle combined heat and power system with integrated thermal energy storage 2017. doi:10.1016/j.applthermaleng.2017.07.163.

[28] Li S, Ma H, Li W. Dynamic performance analysis of solar organic Rankine cycle with thermal energy storage 2018. doi:10.1016/j.applthermaleng.2017.10.021.

[29] Rodríguez JM, Sánchez D, Martínez GS, Ghali Bennouna E, Ikken B. Techno-economic assessment of thermal energy storage solutions for a 1 MWe CSP-ORC power plant. Sol Energy 2016;140:206–18. doi:10.1016/j.solener.2016.11.007.

[30] Patil VR, Biradar VI, Shreyas R, Garg P, Orosz MS, Thirumalai NC. Techno-economic comparison of solar organic Rankine cycle (ORC) and photovoltaic (PV) systems with energy storage. Renew Energy 2017;113:1250–60. doi:10.1016/j.renene.2017.06.107.

[31] Concentrating Solar Power Projects - Saguaro Power Plant | Concentrating Solar Power | NREL n.d. https://www.nrel.gov/csp/solarpaces/project_detail.cfm/projectID=24 (accessed December 6, 2017).

[32] Chambers T, Raush J, Russo B. Installation and operation of parabolic trough organic Rankine cycle solar thermal power plant in south Louisiana. Energy Procedia 2014;49:1107–16. doi:10.1016/j.egypro.2014.03.120.

[33] Italgen Italcementi group. Italgen CSP AIT BAHA Pilot Plant. Integr. Renew. energy Solut. Mediterr. Electr. Mark., Milano: 2014.

[34] Concentrating Solar Power Projects - Rende-CSP Plant | Concentrating Solar Power | NREL n.d. https://www.nrel.gov/csp/solarpaces/project_detail.cfm/projectID=4288 (accessed December 6, 2017).

[35] Yogi D, Co-Pis G, Stefanakos E, Rahman MM, Aydin S, Reedy R, et al. UNIVERSITY OF SOUTH FLORIDA Design, Construction and Operation of CSP Solar Thermal Power Plants in Florida n.d.

[36] Archimede | Case Histories | TURBODEN n.d. https://www.turboden.com/case-histories/1948/archimede (accessed December 6, 2017).

[37] Wendt DS, Mines GL, Turchi CS, Zhu G, Cohan S, Angelini L, et al. Stillwater Hybrid Geo-Solar Power Plant Optimization Analyses Enel Green Power North America, Andover MA 4 Enel Green Power — Innovation Div. GRC Trans 2015;39.

[38] Concentrating Solar Power Projects - Aalborg CSP-Brønderslev CSP with ORC project | Concentrating Solar Power | NREL n.d. https://www.nrel.gov/csp/solarpaces/project_detail.cfm/projectID=8316 (accessed December 6, 2017).

[39] Camerada M, Cau G, Cocco D, Damiano A, Demontis V, Melis T, et al. A Pilot Power Plant Based on Concentrating Solar and Energy Storage Technologies for Improving Electricity Dispatch. Energy Procedia 2015;81:165–72. doi:10.1016/j.egypro.2015.12.071.

[40] ORC-PLUS - Dispatchable small-scale solar thermal electricity n.d. http://www.orc-plus.eu/ (accessed April 4, 2017).

[41] Concentrating Solar Power Projects - eCare Solar Thermal Project | Concentrating Solar Power | NREL n.d. https://www.nrel.gov/csp/solarpaces/project_detail.cfm/projectID=268 (accessed December 6, 2017).

[42] Cocco D, Migliari L, Petrollese M. A hybrid CSP–CPV system for improving the dispatchability of solar power plants. Energy Convers Manag 2016;114:312–23. doi:10.1016/j.enconman.2016.02.015.